Chiral coupling in gold nanodimers

H. Husu,[1,a)] B. K. Canfield,[1] J. Laukkanen,[2] B. Bai,[2] M. Kuittinen,[2] J. Turunen,[2] and M. Kauranen[1]
[1]*Department of Physics, Optics Laboratory, Tampere University of Technology, P.O. Box 692, FI-33101 Tampere, Finland*
[2]*Department of Physics and Mathematics, University of Joensuu, P.O. Box 111, FI-80101 Joensuu, Finland*

(Received 8 August 2008; accepted 18 October 2008; published online 6 November 2008)

Second-harmonic generation from T-shaped gold nanodimers with nanogaps has different efficiencies for left- and right-hand circularly polarized fundamental light. The difference arises from the chiral symmetry breaking of the dimers due to nonorthogonal mutual orientations of the horizontal and vertical bars of the T shape and depends on the gap size. Unexpectedly, the smallest gap with presumably the strongest coupling gives rise to only a small difference. All results can be explained by considering the distribution of the polarized local field in the structure. © *2008 American Institute of Physics*. [DOI: 10.1063/1.3021017]

Metal nanostructures show great prospects for nanophotonic applications such as nanoantennas,[1] nanolenses,[2] nanoscale waveguides,[3] and metamaterials.[4,5] Such applications are often based on the nanostructures' ability to concentrate high local electromagnetic fields, allowing, for example, single-molecule detection by surface-enhanced Raman scattering.[6] Strong fields are particularly important for nonlinear optical processes, which scale with a high power of the field. Four-wave mixing, a third-order process, has been shown to be enhanced by strong fields localized in the gap between two nanoparticles that form a nanodimer.[7] Second-order processes, on the other hand, require also noncentrosymmetry.[8] Thus, second-harmonic generation (SHG) from noncentrosymmetric T-shaped nanodimers is not primarily driven by strong gap fields. Instead, the symmetry of the local field distribution plays the key role.[9]

Symmetry issues are closely associated with the polarization dependence of the optical responses. For example, anisotropic metal nanoparticles exhibit dichroism, i.e., their response is different for two orthogonal polarizations.[10] In addition, chiral nanostructures may exhibit high optical activity with polarization rotations of up to $10^4°/\mathrm{mm}$.[11,12] In general, chirality arises from the lack of reflection symmetry in the sample. Because of the noncentrosymmetry requirement, second-order processes are particularly sensitive tools to study such symmetry-breaking effects even when traditional linear techniques would reveal no effect. The symmetry of nanostructured samples may be broken by their overall features or small-scale defects. We have already shown that symmetry breaking due to small defects can play an important role in the second-order response of metal nanostructures[13] and can lead to strong inhomogeneous effects in the nonlinear responses.[14]

In this letter, we show that SHG from T-shaped gold nanodimers is significantly influenced by the chiral symmetry breaking that arises from the nonorthogonal mutual orientations of its horizontal and vertical bars. In particular, the responses differ for left- and right-hand circularly polarized (LCP and RCP, respectively) fundamental light. Because of the symmetry of the individual bars, such effects must arise from their mutual coupling. One would therefore expect that the smallest gap should lead to the strongest coupling and thus the highest chiral signatures. In contrast to this, our results show that the chiral signatures for the smallest gaps are weak and that they peak for a larger gap size. The results can be explained by considering the polarization-dependent local field distribution of the fundamental light in the structure for LCP and RCP.

Several arrays of T-shaped gold nanodimers were fabricated on a fused silica substrate using electron beam lithography and lift-off processes.[9] The horizontal and vertical bars were separated by different gap sizes ranging from very small (nominally 2 nm) to 40 nm. All the bars were designed to be 250 nm long, but the fabrication process resulted in some variation in the lengths. The linewidth of the bars is approximately 125 nm, the thickness of the gold layer is 20 nm, and the array period is 500 nm. Finally, the samples are protected by a 20 nm thick layer of fused silica. The two bars forming the T shape were designed to be orthogonally oriented so that the ideal T shape has a mirror plane along the vertical bar. However, due to the imperfections in the fabrication process, the mutual orientations of the bars are slightly slanted (Fig. 1). The slant is not constant but varies from 0° to 5° between different dimers. According to scanning electron microscope (SEM) images one can estimate an

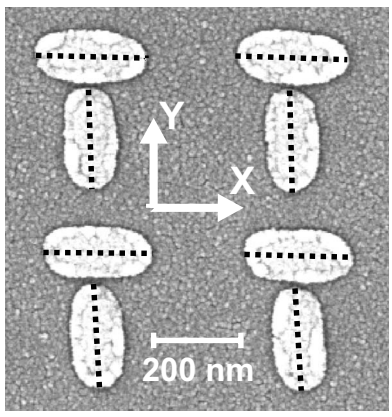

FIG. 1. SEM image of a sample with a 15 nm gap. Dashed lines emphasize the slant of the bars.

a)Electronic mail: hannu.husu@tut.fi.

average slant of 3°. The slant breaks the ideal symmetry and thus makes our samples chiral.

Our experiments, to be described below, are performed at normal incidence. We therefore describe the second-harmonic (SH) response using the macroscopic nonlinear response tensor that connects the polarization components of the incoming fundamental beam to those of the SH signal as

$$E_I(2\omega) = \sum_{J,K} A_{IJK} E_J(\omega) E_K(\omega), \tag{1}$$

which obeys electric-dipole-type selection rules.[15]

For collimated beams with in-plane (X,Y) polarization components, an ideal T sample has four nonvanishing tensor components IJK: YYY, YXX, $XXY=XYX$. Due to the mutual slant of the bars, a real T shape has four additional (ideally forbidden) tensor components: $YYX=YXY$, XXX, and XYY, which are thus associated with chiral symmetry breaking of the sample.

The output field at the SH frequency can be presented with the equation

$$E_I(2\omega) = A_{IXX} E_X^2(\omega) + A_{IYY} E_Y^2(\omega) + 2A_{IXY} E_X(\omega) E_Y(\omega), \tag{2}$$

where $I=X$, Y.[15] For circularly polarized fundamental light $E_Y(\omega) = \pm i E_X(\omega)$, and the Y-polarized SH field, for example, is found to be $E_{Y,CP}(2\omega) = (A_{YXX} - A_{YYY} \pm i2A_{YXY}) E_X^2(\omega)$.

For an ideal achiral T shape, the tensor component A_{YXY} is zero, and thus there is no difference in the SH fields for LCP and RCP. However, for a chiral sample the additional tensor components lead to different SH fields and therefore also different SH intensities for LCP and RCP. Such a circular-difference response (CDR) therefore arises from interference between the allowed and forbidden tensor components and is defined as a difference between the SH intensities for LCP and RCP divided by the average of the intensities,[16]

$$\mathrm{CDR} = \left| \frac{I_{\mathrm{LCP}} - I_{\mathrm{RCP}}}{(I_{\mathrm{LCP}} + I_{\mathrm{RCP}})/2} \right|. \tag{3}$$

Note that the CDR can take values between 0 and 2. In the following, we take CDR as the measure of the chirality arising from the coupling between the bars of the T dimer.

SHG measurements were performed in transmission at normal incidence using a Nd:glass laser (wavelength of 1060 nm, pulse length of 200 fs, repetition rate of 82 MHz, and average power of 300 mW) as the source of fundamental light. The diameter of the focal spot is 200 μm, so there are about 10^5 dimers within the spot area. The optical densities of all samples at 1060 nm are very close to each other, and therefore the differences in the measurement results cannot be explained by the differences in the linear response of the samples.[9]

Different polarization states of the fundamental beam are addressed by continuously varying the state of polarization of the fundamental beam with a quarter waveplate (QWP). To keep the measurement system fairly simple and to avoid handedness of the setup itself, no specific output polarization was detected. An example measurement curve is illustrated in the inset of Fig. 2. Such measurements also give the SH intensities for LCP and RCP fundamental light, which are obtained with QWP angles of 45° and 135°, and subsequently the values of the CDR. In order to reduce the uncertainty of the results used to calculate the CDRs, the SH intensity values were determined by fitting the measurement data to a theoretical model based on Eq. (2).[15]

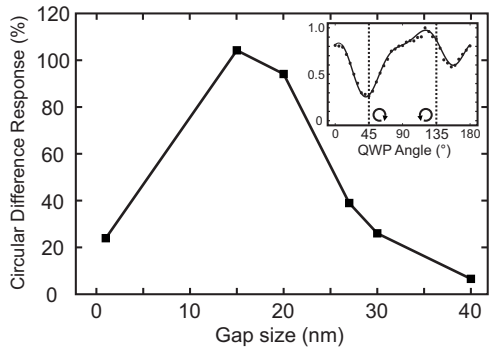

FIG. 2. CDR as a function of gap size. Inset: Normalized SHG intensity from a sample with a 15 nm gap as a function of the QWP angle. The solid curve is a fit to a theoretical model based on Eq. (2). Vertical dashed lines indicate the circular polarization states.

CDR values as a function of gap size are shown in Fig. 2. In general, the CDR decreases with increasing gap size, which corresponds to the fact that the chirality arises from the interaction between the bars. The general trend also reveals that the influence of small-scale defects in the particles is less important. Surprisingly, however, the smallest gap exhibits a very small CDR. We note that the allowed SH signals from the T samples have been earlier explained by considering the symmetry of the polarized local fundamental field distribution in the structure and its interaction with the surface nonlinearity of the metal-dielectric interfaces.[9] To explain the CDR results, we adapt this approach by considering local field distributions for circular input polarizations (Fig. 3). The calculations are performed using the Fourier modal method,[17] which takes into account also the periodicity, and thus a possible coupling between different dimers of the array.

To obtain qualitative understanding of the experimental results, it is sufficient to consider only the distribution of the local field Y-component because no significant gap dependence appears in the distribution of the X-component. For an ideal sample with no slant, the local field distributions for LCP and RCP are mirror images of each other because of the sample symmetry [Figs. 3(a)–3(d)]. When the vertical bar is slightly slanted, the local field distributions in a sample with a 2 nm gap are not significantly modified [Figs. 3(e) and 3(f)], and the fields also remain relatively weak compared to

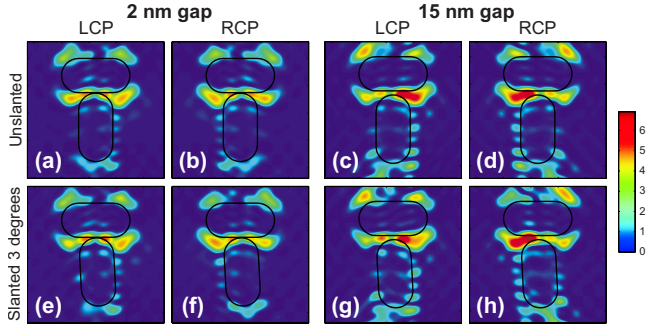

FIG. 3. (Color online) The distribution of the local electric field Y-component for fundamental LCP and RCP. Distributions are presented for gap sizes of 2 and 15 nm. Note that for an ideal sample with no slant, the distributions for LCP and RCP are mirror images of each other.

other gap sizes. Thus, the distributions for LCP and RCP are very similar, leading to a small CDR.

For a 15 nm gap, however, even a small slant of the vertical bar leads to a significant difference in the local fields for LCP and RCP incident light [compare Figs. 3(g) and 3(h)]. Thus, when these fields drive the second-order nonlinear response, which is extremely sensitive to the smallest details, the chiral signature in SHG is large. Furthermore, with larger gap sizes the interaction between the bars becomes weaker, diminishing the effect of the mutual slant. Thus, the CDR decreases as the gap size is increased.

In our earlier work with L-shaped gold nanoparticles, we obtained CDR values from 140% to 180%.[13] In those samples the chirality arises from small-scale defects, which also attract extremely high local fields. In the present T-shaped nanodimers, the chirality arises from the symmetry broken sample geometry. As the SHG is extremely sensitive to the symmetry breaking, even a small slant is sufficient to give rise to a large difference in the SH measurements.

In conclusion, we have investigated the effects of chiral symmetry breaking on the SH response of T-shaped gold nanodimers, in which the horizontal and vertical bars of the T dimer are separated by a small nanogap. A small slant in the mutual orientations of the bars gives rise to different SH responses for the two circular polarizations of the fundamental light. The CDR depends on the gap size, but the dependence is nontrivial. The results are explained well by considering the highly gap-sensitive local electric field distributions for LCP and RCP at the fundamental laser frequency.

We acknowledge the support by the Academy of Finland (Grant Nos. 113245, 114913, and 118357) and by the Nanophotonics Program of the Ministry of Education of Finland. H.H. acknowledges support from the Graduate School of Tampere University of Technology.

[1] P. Muhlschlegel, H. Eisler, O. J. F. Martin, B. Hecht, and D. W. Pohl, Science **308**, 1607 (2005).
[2] K. Li, M. I. Stockman, and D. J. Bergman, Phys. Rev. Lett. **91**, 227402 (2003).
[3] L. A. Sweatlock, S. A. Maier, H. A. Atwater, J. J. Penninkhof, and A. Polman, Phys. Rev. B **71**, 235408 (2005).
[4] T. Pakizeh, M. S. Abrishamian, N. Granpayeh, A. Dmitriev, and M. Käll, Opt. Express **14**, 8240 (2006).
[5] M. W. Klein, C. Enkrich, M. Wegener, and S. Linden, Science **313**, 502 (2006).
[6] K. Kneipp, Y. Wang, H. Kneipp, L. T. Perelman, I. Itzkan, R. R. Dasari, and M. S. Feld, Phys. Rev. Lett. **78**, 1667 (1997).
[7] M. Danckwerts and L. Novotny, Phys. Rev. Lett. **98**, 026104 (2007).
[8] H. Tuovinen, M. Kauranen, K. Jefimovs, P. Vahimaa, T. Vallius, J. Turunen, N. V. Tkachenko, and H. Lemmetyinen, J. Nonlinear Opt. Phys. Mater. **11**, 421 (2002).
[9] B. K. Canfield, H. Husu, J. Laukkanen, B. Bai, M. Kuittinen, J. Turunen, and M. Kauranen, Nano Lett. **7**, 1251 (2007).
[10] W. Gotschy, K. Vonmetz, A. Leitner, and F. R. Aussenegg, Opt. Lett. **21**, 1099 (1996).
[11] E. Plum, V. A. Fedotov, A. S. Schwanecke, N. I. Zheludev, and Y. Chen, Appl. Phys. Lett. **90**, 223113 (2007).
[12] M. Kuwata-Gonokami, N. Saito, Y. Ino, M. Kauranen, K. Jefimovs, T. Vallius, J. Turunen, and Y. Svirko, Phys. Rev. Lett. **95**, 227401 (2005).
[13] B. K. Canfield, S. Kujala, K. Laiho, K. Jefimovs, J. Turunen, and M. Kauranen, Opt. Express **14**, 950 (2006).
[14] B. K. Canfield, H. Husu, J. Kontio, J. Viheriälä, T. Rytkönen, T. Niemi, E. Chandler, A. Hrin, J. A. Squier, and M. Kauranen, New J. Phys. **10**, 013001 (2008).
[15] B. K. Canfield, S. Kujala, K. Jefimovs, Y. Svirko, J. Turunen, and M. Kauranen, J. Opt A, Pure Appl. Opt. **8**, S278 (2006).
[16] M. Kauranen, T. Verbiest, and A. Persoons, J. Mod. Opt. **45**, 403 (1998).
[17] L. Li and J. Opt, Pure Appl. Opt. **5**, 345 (2003).